Application of Surfactant Modified Kono-Boue Clay Nanopartices in Oil Recovery

Abstract

Sodium Dodecyl Sulphate (SDS) mediated Kono-Bono (KB) clay nanoparticles (NPs) applied in Enhanced Oil Recovery (EOR) has been investigated for the first time. This was done using synthesized KB clay NPs as control and SDS treated KB clay NPs experiments in a micro model to determine the rate of oil recovery. The samples were prepared by dissolving 15 g of KB clay in a mixture of 450 ml of de-ionized water and 150 ml of varying SDS concentrations, magnetically stirred, dried at 110 °C for 90 minutes and further calcined at 900 °C in a muffle furnace for 120 minutes. The samples were characterized with Fourier Transform Infra-red (FT-IR) Spectroscopy, Scanning Electron Microscopy (SEM), X-ray fluorescence (XRF) and X-ray Diffraction (XRD), respectively. FT-IR analysis indicated characteristic bending vibrations of Al-OH bands at 698 cm^{-1} and stretching modes at 780, 1056 and 3655 cm^{-1} for (Si-O and Al-Mg-OH) bands respectively. SEM micrographs showed surfaces with varying platy polycrystalline particle sizes while XRF results identified the clay as kaolinite with silicate and alumina > 30 and 16%, respectively. Flooding experiment conducted revealed that the SDS mediated KB clay NPs (with 8.33 mM SDS) gave the highest total oil recovery of 66.25 % at 0.10 wt. %. Optimizing oil recovery at 8.33 mM by varying concentrations of KBC2 at 0.05, 0.10, 0.15, 0.20 and 0.25 wt. % gave a remarkable oil recovery rate of 85.27% at 0.15 wt.%. Thus, 0.15 wt. % KBC2 is recommended for application in oil recovery.

Keywords: Enhanced Oil Recovery, Kono-Boue Clay, Micro model, Nanoparticles, SDS-Mediated.

Introduction

Crude oil can be recovered from trapped/depleting oil reserves especially in this era of high population and consequently increased energy demand. Oil can be recovered using conventional methods (primary and secondary) by employing natural reservoir pressure flow/assisted lift such as gas cap drive, gravity drainage, solution drive, water drive and maintaining the reservoir pressure as a result of pressure drop via gas and water injection [1, 2]. These methods still leave a high percentage of oil trapped in the oil reserves possibly due to high energy at the water-oil interface and heterogeneity of the reservoir.

Several tertiary recovery methods, also known as EOR have been employed to displace more oil and improve recovery efficiency [3, 4]. Some of the tertiary methods utilize chemicals [5], heat [6], gas [7] or microbes [8] to enhance the displacement of oil. Researches have shown that Chemical Enhanced Oil Recovery (CEOR) using surfactants such as Cetyltrimethylammonium bromide (CTAB), a cationic surfactant [9], Triton X-100 (TX-100) a nonionic surfactant [10], Pickering emulsions involving nonionic surfactants (cetyl polyoxyethylene ether-C16E20) [11] and anionic surfactant, Sodium dodecyl sulphate (SDS) with silica nanoparticless[12] have been successful and are effective in oil displacement. Some mechanisms employed are reduction of the capillary force and thus the interfacial reduction, lowering the viscosity of oil and also modifying the wettability of the formation towards a more water wet condition [13-15].

Clays are minerals majorly comprising of hydrated aluminum and/or magnesium phyllosilicates [16]. Clays can be modified to enhance their properties which can be beneficial in many applications such as textile industry [17], catalyst [18], medicine, pharmacy [19], cosmetics [20], food packaging and oil industry [21-23]. Cheraghian *et al*. [22] reported that oil recovery improved by flooding with clay (local sodium bentonite) NPs and SDS solution. Oil increment up to 52% was obtained when nanoclay particles with SDS solution of 1800 ppm was utilized in flooding [22]. Employing cheaper local materials such as clay with similar properties as some NPs such as silica NPs has made the use of clay an economically viable option among others.

Gbarakoro *et al*. [18] reported that KB clay possessed kaolinite clay structure with aluminum to silica ratio of 1:4. Furthermore, Udeh *et al*. [24] successfully studied the interactions and stability of foam generated from SDS mediated KB clay NPs and reported that SDS mediated KB clay NPs via sol-gel route significantly led to particle size variation of the modified clay NPs. These variations created porous spaces in the modified clay matrices and the batch with the least particle size achieved the most stable foam. However, no work has been done on its application in EOR. This work seeks to investigate the application of SDS mediated KB clay NPs at varying SDS concentrations using the sol-gel route and the extent of recovery via micro model for the first time.

2.0 Materials and Methods

2.1 Materials

KB clay particles were collected from Kono-Boue in Khana Local Government Area, Rivers State, Nigeria. Other materials used were crude oil gotten from Obelle well 5, Obelle flow station, Port Harcourt, Rivers State with 31.14 °API, at 29 °C. Oil viscosity and density were 10.4832 cP and 0.8704 g/ml, respectively. Sandstone core samples were washed with distilled water and ethanol to remove impurities and water respectively; they were dried at 90 °C in an oven

for 24 hours. The reagents and equipment used in the flooding experiment were:- 99.9% pure Sodium Dodecyl Sulphate (SDS) ($C_{12}H_{24}SO_4Na$, M.W. = 288.38 g/mol) purchased from British drug House, UK, sodium chloride salt, distilled water, micro model, weighing balance, magnetic stirrer/bar, oven, and muffle furnace.

Table 1. Properties of core samples

Length (cm)	0.38
Diameter (cm)	0.24
Bulk volume (cm^3)	300
Mass of dry sample (kg)	1.250
Mass of saturated sample (kg)	1.580
Mass of water (g)	330
Porosity (%)	35.00
Pore Volume (cm^3)	105

2.2 Methods

2.2.1. Synthesis of Clay NPs

Clay particles were dried in an oven at 120 °C for 3 hours for all moisture to be completely evaporated. They were further ground and sieved with a mesh sieve of size 1.00 mm. 15 g of fine clay grains were dissolved in 450 ml of distilled water and stirred magnetically for 90 minutes. The water in the mixture was decanted and further washed three times, oven dried for 1 day at 110 °C. The dried particles were calcined in a muffle furnace at 900 °C for 120 minutes.

2.2.2. Synthesis of SDS Mediated Clay NPs

Varying SDS concentrations of 2, 8, and 14 mM were prepared by dispersing 0.15 g, 0.60 g, and 1.05 g, respectively in 200 ml of distilled water and made up to 250 ml mark. Same procedure was used in the preparation of SDS mediated clay NPs but different concentrations of SDS solutions of 2, 8 and 14 mM was used in place of distilled water.

2.2.3. Clay Nanofluid Preparation

The clay nanofluids were prepared by dispersing 0.1 wt. % of various synthesized clay NPs in 100 ml volume of distilled water.

2.2.4. Characterization

The analysis of synthesized samples was done using Fourier Transform Infra-red (FT-IR) (Agilent Technology Cary 630 FTIR), X-Supreme 8000 X-ray Fluorescence (XRF), Scanning Electron Microscope (SEM) and X-ray Diffraction (XRD) EMPYREAN diffractometer, with a Cu Kα radiation of λ=0.15406 nm and Cu anode current and voltage of 40 mA and 45kV respectively to determine functional groups, the elemental composition, surface morphologies of the samples and the crystal structures, respectively. FTIR samples were prepared by mixing a small spatula of it with KBr and pelletizing the mixture with an IR press before analysis. Both XRF and XRD samples were ground using mortar and pestle before placing on a sample holder for analysis. In the case of XRF, 2 g of the ground sample was vacuum-dried for 10 minutes and allowed to run for 10 minutes in the XRF spectrometer while XRD sample was ran without further pretreatment.

SEM samples were used without grinding. Small particles of each were placed on a sticky pad on top of an aluminum stub screwed in a sample holder and slotted into the SEM for analysis.

2.2.5. Flooding Experiments

Experiments were done with core samples in a micro model. The primary and secondary flooding experiments were conducted by flooding the oil-wet core samples with 3% wt. brine solution. This was after the core samples were first saturated with brine solution to ensure initial water saturation and injection of three pore volumes of crude oil, left for 2 days to establish oil-wet condition. Three pore volumes each of the prepared clay nano fluid for control and SDS treated were used in flooding to determine the rate of oil displacement. Each flooding experiment was completed by injecting two pore volumes of brine. This was done for the four different SDS concentrations at 0, 2, 8 and 14 mM and the values of oil recovered after each experiment was recorded. The flooding experiments were performed at a pressure of 5 psi at 29 °C. The mean values of oil and water recovered was recorded.

The oil saturations (residual and critical), total oil recoveries and displacement efficiencies were calculated using the equations (1-3) respectively.

$$\text{Residual Oil Saturation} = \frac{\text{Original Oil in Place}}{\text{Pore Volume}} \times 100 \quad (1)$$

$$\text{Critical Oil Saturation} = \frac{\text{Volume of oil left after water injection}}{\text{Pore Volume}} \times 100 \quad (2)$$

$$\text{Displacement Efficiency} = 1 - \left[\frac{\text{Original Oil in Place}}{\text{Pore Volume}} \times 100\right] \quad (3)$$

3.0 Results and Discussion

3.1 Characterization

3.1.1 FT-IR

The FT-IR spectra of the control experiment (KBC0) and SDS mediated clay NPs (KBC1, KBC2 and KBC3) were analyzed within the band ranges of 4000 – 650 cm^{-1}. The absorption bands shown in Fig. 1 and Table 2 consist of absorption peaks for Si-O vibrational stretching at 1052 - 1056 cm^{-1} and 780 cm^{-1} which correspond to bands associated with the presence of silicate layers such as kaolinite [25-29]. The band at 698 cm^{-1} was assigned to Al-OH bending while absorption peaks at 3655 and 3555 cm^{-1} correspond to Al/Mg-O-H Stretching vibrations [25, 28].

Table 2. FT-IR of KBC0, KBC1, KBC2 and KBC3

KB Clay NPs Ctrl (KBC0)	KB Clay NPs 2 mM (KBC1)	KB Clay NPs 8 mM (KBC2)	KB Clay NPs 14 mM (KBC3)	Assigned Absorption Band

3655	3555	-	3655	Al/Mg-O-H Stretching
1056	1056	1056	1052	Si-O Stretching
780	780	780	780	Si-O Stretching
698	695	698	698	Al-OH bending

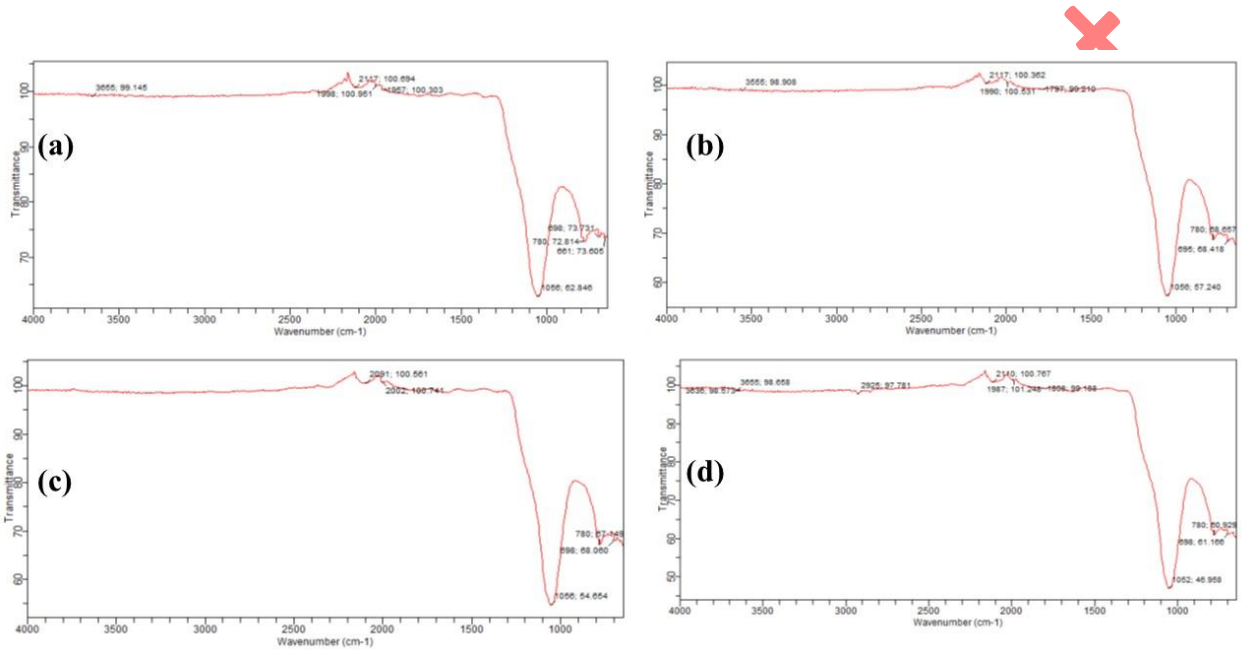

Fig.1. FT-IR spectra for (A) KBC0, (B) KBC1, (C) KBC2 and (D) KBC3.

3.1.2 SEM

The SEM micrographs for the clay NPs (control experiment) and SDS mediated clay NPs (Fig. 2) were taken at 1000 magnification (1000X) with scale bar of 268 µm (for ease of comparison). The surface morphologies show that the samples form polycrystallite aggregates in platy forms. More porous aggregates were observed in SDS mediated clay NPs (KBC1, KBC2 and KBC3) than the control (KBC0). The smallest-sized particles were observed in KBC2 which was prepared with the SDS solution at CMC (8.33 mM) [29].

3.1.2 XRD

The XRD diffraction patterns for KBC0, KBC1, KBC2 and KBC3 are shown in Fig 3. The presence of two major peaks at 2θ, 21° and 27° agreed with kaolinite structure of KB clay reported by Gbarakoro *et al*. [18]. The average particle size estimated from the Scherrer's formula using the XRD data also confirmed that particles of KBC2 had the least particle size [24].

3.1.3 XRF

The elemental compositions of the samples are shown in Table 3 with major elements such as Si and Al having approximately 30% and greater than 16% respectively, confirming the KB

clay NPs as kaolinites. Other minor elements like Mg, Fe and few trace elements of S, Ti and K were also observed [18].

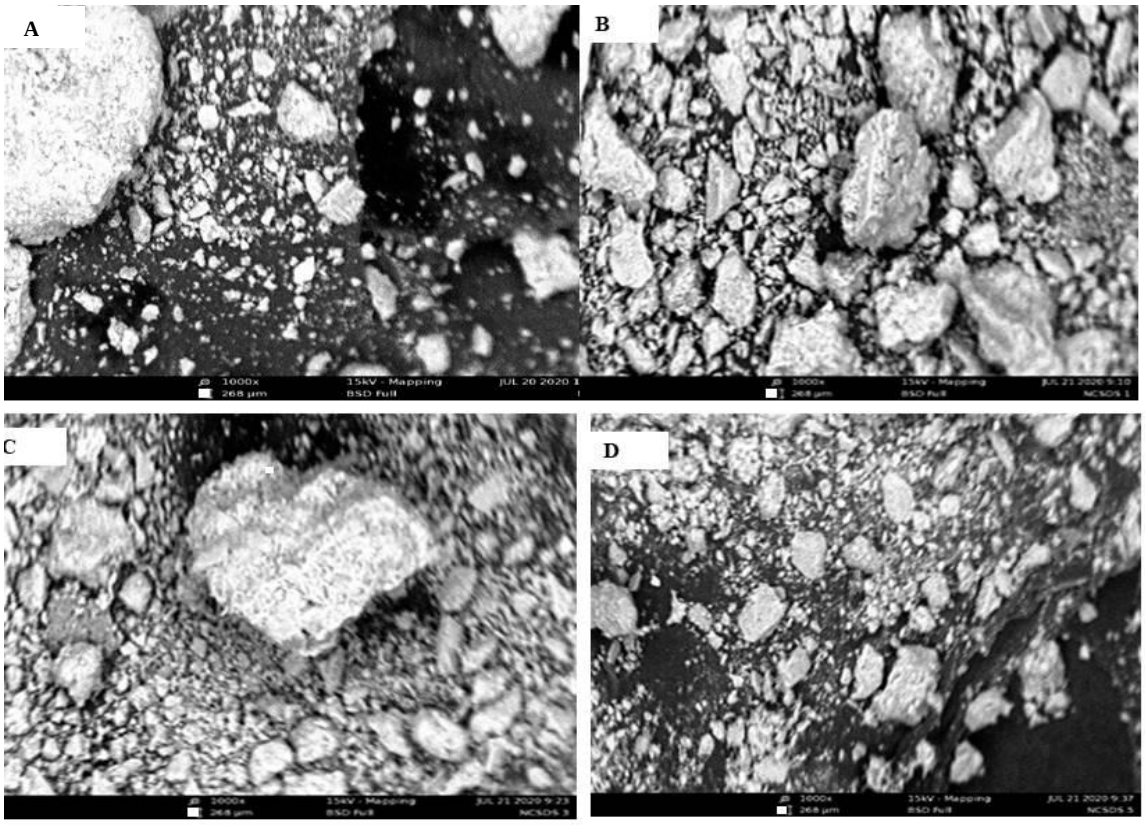

Fig. 2. Surface morphologies of (A) KB Clay NPs Control (B) KB Clay NPs 2mM (C) KB Clay NPs 8mM (D) KB Clay NPs 14mM

Table 3. Percentage Elemental Composition of KBC0, KB1 and KBC3

Elements (%)	KBC0	KBC1	KBC3
Si	30.10	29.83	29.38
Al	16.96	16.19	16.15
Fe	2.34	2.20	2.18
Mg	2.09	1.76	2.34
S	0.04	0.20	0.29
Ti	0.81	0.77	0.78
K	0.95	0.93	0.93
Si/Al	1.78	1.84	1.82

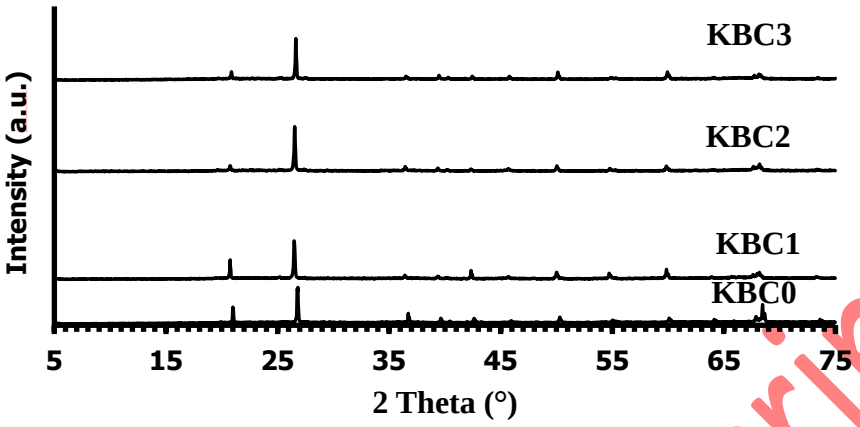

Fig. 3. XRD of KBC0, KBC1, KBC2 and KBC3

3.2 Micromodel Results

Oil saturations as well as total oil recoveries are terms used to discuss the displacement of oil from core samples in the model. Flooding the model with equal pore volumes of brine solution gave residual oil saturations as presented in Table 4 denoting the oil percentage left after primary and secondary flooding. Close results of residual oil saturations for both the mediated (control and SDS treated) clay NPs suggest similar flooding properties and represents the conventional method of oil recoveries [30]. However, flooding the model with the four prepared clay nanofluids (KBC0. KBC1, KBC2 and KBC3) showed a decrease/reduction in oil saturation from higher residual saturation to relatively lower critical oil saturation values. [31] This suggests that the synthesized KB clay NPs interacted with oil/rock and favourably modified the properties of the oil (Fig. 4).

It could be attributed to the recovery mechanisms which includes lowering of the capillary force between water and oil leading to reduction in the interfacial tension, alteration in rock wettability from oil-wet towards water wet condition [31][32]. The displacement of oil from trapped oil pockets is also achieved as oil viscosity reduces [15, 32,33]. The displacement of oil was mostly achieved in KBC2 as clearly shown in EOR efficiency of 21.91% as against those obtained with KBC0, KBC1 and KBC3 which were 8.58%, 19.39% and 12.77%, respectively (Fig. 4 and 5). The EOR efficiency of KBC2 was also greater than 20% reported in recent literature [12]. This could be as a result of more particle aggregation on the surface of KBC2 (Fig. 2C), probably due to the exit of SDS which left numerous porous spaces on the surface during calcination and subsequently resulted in particle size variation.

The result is in line with the report analyzed by Udeh *et al* [24]. The small sized particles could penetrate more into tiny porous spaces, displacing the oil passed by water, yielding a total oil recovery of 66.25%. Additionally, KBC2 had the SDS concentration at the CMC which is in agreement with the report by Cheraghian and Seyyed [22]. The optimum total oil recovery of KBC2 was determined by varying its concentrations as 0.05, 0.10, 0.15, 0.20 and 0.25 wt. %. This optimization process gave the highest recovery of 85.27% at 0.15 wt. % and at constant SDS concentrations of 8 mM (Fig. 6). This could be attributed to increase in the concentration of KBC2 which made the interface to adsorb more NPs and exerts pressure on the oil droplets. Such process could lower the IFT and significantly alters the wettability from more oil wet towards more water

wet condition resulting in enhancement of the efficiency of the recovery process. However, the decrease in efficiency observed after 0.15 wt. % could be linked to log jamming of NPs accumulation causing pore throat blockage [32].

3.2.1 Oil Saturations

Table 4. Fluid Saturations of KB Clay/SDS nanofluids

KB Clay/SDS nanofluids	Residual Oil Saturation (%)	Critical Oil Saturation (%)
KBC0	58.48	49.90
KBC1	56.22	36.83
KBC2	55.66	33.75
KBC3	57.92	45.15

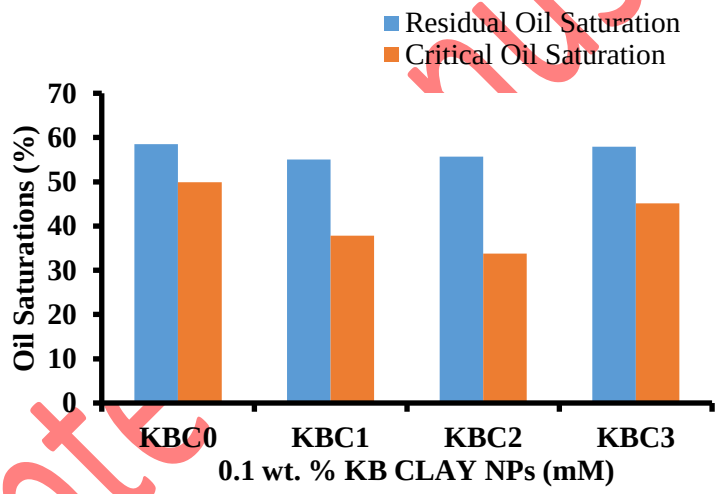

Fig. 4. Oil Saturations of 0.1 wt. % KB Clay NPs

Table 5. Oil Recoveries of KB Clay SDS Mediated NPs

SDS-mediated clay NPs	1° & 2° recovery (before application) (%)	3° (EOR) (after application) (%)	Total Oil Recovery (%)	Displacement Efficiency (%)
KBC0	41.52	8.58	50.1	14.67
KBC1	43.78	19.39	63.17	34.49
KBC2	49.34	21.91	66.25	39.36
KBC3	42.08	12.77	54.85	22.05

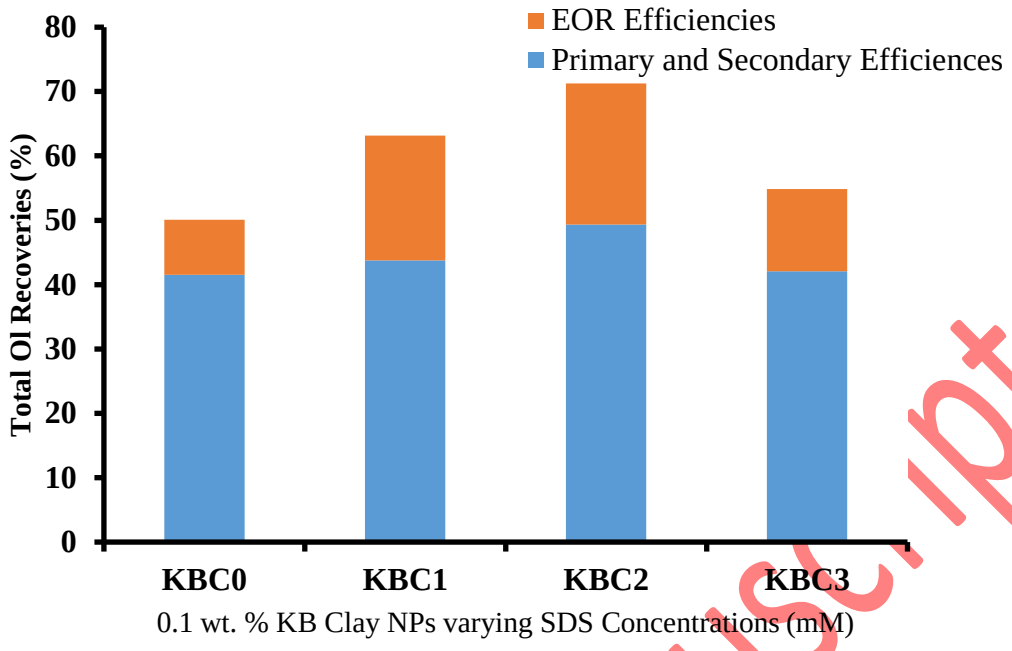

Fig. 5. Total Oil Recoveries of 0.1 wt. % KB Clay NPs

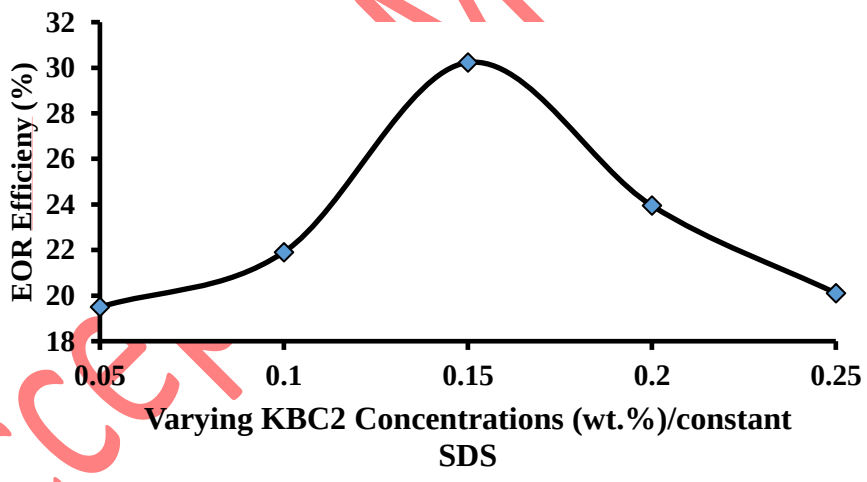

Fig. 6. EOR Efficiency for Optimized KBC2 Concentrations

Conclusion

SDS- mediated KB clay NPs has been synthesized, characterized and the resultant nanofluids employed in flooding in oil recovery experiment for the first time. The XRD pattern confirmed the KB clay as having kaolinite structure while the FT-IR analysis obtained showed stretching and bending vibrations of Si-O and Al-OH at 780, 1056 and 698 cm^{-1} respectively. SEM results showed polycrystallites in platy forms while the XRF results confirmed the silica and alumina as having the highest percentages of Si > 30 and Al > 16%, respectively. Experiments on core flooding showed total oil recovery of 66.25 % with an EOR efficiency of 21.91 % obtained

by flooding 0.1 wt. % of KBC2 with 8.33 wt. % SDS and applying optimized approach by varying KBC2 concentrations gave a record high recovery efficiency of 85.27% at 0.15 wt.%.

Acknowledgement

The authors of this work sincerely thank the Tertiary Educational Trust Fund (TETFUND) for the financial support provided during this research through Institution Based Research (IBR) Grant of Rivers State University, Port Harcourt, Nigeria and the Umaru Musa Yar'adua University Central Research Laboratory for the XRD, SEM, FT-IR and XRF analyses.

References

[1] Omar C. Innovation in Enhanced Oil Recovery. Recent Advances in Petrochemical Science. 2018; 5(2). DOI: 10.19080/RAPSCI.2018.05.555659

[2] Massarweh O, Abushaikha, AS. The use of surfactants in enhanced oil recovery: A review of recent advances. Energy Reports. 2020;6:3150–3178. https://doi.org/10.1016/j.egyr.2020.11.009

[3] Li K, Wang D, Jiang S. Review on enhanced oil recovery by nanofluids. Oil & Gas Science and Technology – Revue d' IFP Energies nouvelles. 2018;73(37) https://doi.org/10.1051/ogst/2018052.

[4] Brantson ET, Ju B, Appau PO, Akwensi PH, Peprah GA, Liu N, Aphu ES, Boah EA, Borsah AA. Development of hybrid low salinity water polymer flooding numerical reservoir simulator and smart proxy model for chemical enhanced oil recovery (CEOR). Journal of Petroleum Science and Engineering. 2020;187,106751. http://dx.doi.org/10.1016/j.petrol.2019.106751.

[5] Pothula GK, Vij RK, Bera A. An overview of chemical enhanced oil recovery and its status in India. Petroleum Science. 2023;20(4): 2305-23.

[6] Mokheimer EMA, Hamdy M, Abubakar Z, Shakeel MR, Habib MA, Mahmoud M. A comprehensive review of thermal enhanced oil recovery: Techniques evaluation. Journal of Energy Resources Technology. 2019;141(3):030801. http://dx.doi.org/10/1115/1.4041096.

[7] Song ZJ, Li M, Zhao C, Yang YL, Hou JR. Gas injection for enhanced oil recovery in two-dimensional geology-based physical model of Tahe fractured-vuggy carbonate reservoirs: karst fault system. Petroleum Science. 2020;17:19-33

[8] Niu J, Liu Q, Lv J, Peng B. Review on microbial enhanced oil recovery: Mechanisms, modeling and field trials. Journal of Petroleum Science and Engineering. 2020;192,107350. http://dx.doi.org/10.1016/j.petrol.2020.107350.

[9] Shahbazi S, Goodpaster JV, Smith GD, Becker T, Lewis SW. Preparation, characterization and application of a lipophilic coated exfoliated Egyptian blue for near- infrared luminescent latent fingermark detection. Forensic Chemistry, 2020;18,100208. http://dx.doi.org/10.1016/j.forc2019.100209.

[10] Hosseini S, Experimental investigation of effect of asphaltene deposition on oil relative permeability, rock wettability alteration and oil recovery in WAG process. Petroleum Science and Technology. 2019;37(20):2150-2159. http://dx.doi.org/10.1080/10916466.2018.1482335.

[11] Yang L, Ge J, Wu H, Li X, Li J, Zhang G. Study on the Enhanced Oil Recovery Properties of the Pickering Emulsions for Harsh Reservoirs. ACS Omega. 2024; DOI: 10.1021/acsomega.4c06834

[12] Wu Y, Chen W, Dai C, Huang Y, Li H, Zhao M, He L, Jiao B. Reducing surfactant adsorption on rock by silica nanoparticles for enhanced oil recovery. Petroleum of Science and Engineering. 2017;153, 283-287. http://dx.doi.org/10.1016/j.petrol.2017.04.015.

[13] El-hoshoudy AN, Desouky SEM, Elkady MY, Al-Sabagh AM, Betiha MA, Mahmoud S. Hydrophobically associated polymers for wettability alteration and enhanced oil recovery – Article review. Egyptian Journal of Petroleum. 2017; 26(3): 757–762. http://dx.doi.org/10.1016/j.ejpe.2016.10.008.

[14] Zhu D, Hou J, Wang J, Wu X, Wang P, Bai B. Acid-alternating base (AAB) technology for blockage removal and enhanced oil recovery in sandstone reservoirs. Fuel. 2018; 215: 619–630. http://dx.doi.org/10.1016/j.fuel. 2017.11.090.

[15] Almubarak M, Alyousef Z, Almajid M, Almubarak T, Ng JH. Enhancing foam stability through a combination of surfactant and nanoparticles. In: Abu Dhabi International Petroleum Exhibition and Conference. 2020; https://doi.org/10.2118/202790-MS. OnePetro.

[16] Gamoudi S, Srasra E. Modification of Clay Minerals by Surfactant Agents: Structure, Properties and New Applications. InSurfactants-Fundamental Concepts and Emerging Perspectives. 2024, doi: 10.5772/intechopen.110317.

[17] Choi YS, Cho JH. Color removal dyes from wastewater using vermiculite. Environmental Technology. 1996;17:1169-1180.

[18] Gbarakoro SL, Konne JL, Boisa N. Characterization of Kono-Boue clay as possible catalyst for biodiesel production. International Journal of Science and Research (IJSR), 2016;5(6):924-928. http://dx.doi.org/10.21275/v5i6.NOV164059.

[19] Selvasdha N, Dhanalekshmi UM, Krishnaraj S, Harish Sundar Y, Sri Durga Devi N,Sarathchandiran I. Multifunctional Clay in Pharmaceuticals . InClay Science and Technology. 2021; http://dx.doi.org/10.5772/intechopen.92408.

[20] Moraes JD, Bertilino R, Cuffini SL, Ducart DF, Bretzke PE, Leonardi GR. Clay minerals: Properties and applications to dermocosmetic products and perspectives of natural raw materials for therapeutic purposes- A review. International journal of pharmaceutics. 2017; 534(1-2):213-9.

[21] Gbarakoro SL, Konne JL, Ofodile S. Synthesis and Evaluation of Biodiesel Using Calcined and Acid Modified Kono-Boue Clays as Catalyst, International Journal of Chemistry and Chemical Processes. 2018; 4(1): 2545 – 5265.

[22] Cheraghian G, Seyyed SK. Improvement of heavy oil recovery and role of nanoparticles of clay in the surfactant flooding process, Petroleum Science and Technology, 2016; 34(15): 1397-1405, DOI: 10.1080/10916466.2016.1198805

[23] Naman K, Sudhanshu S. Exfoliation and Extraction of Nanoclay from Montmorillonite Mineral Rich Bentonite Soil,IACMAG_Symposium. 2020;56.https://doi.org/10.1007/978-981-15-0890-5_1

[24] Udeh OV, Konne JL, Cookey GA, Nmegbu GJC. Foam Stabilization and Interactive Properties of Kono-Boue Clay Nanoparticles in Oil Recovery. Journal of Chemical Society of Nigeria. 2022; 47(4).https://doi.org/10.46602/jcsn.v47i4.799

[25] Nandiyanto ABD, Oktiano R, Ragadhita R.(2019), How to Read and Interpret FTIR, Spectroscope of Organic material, Indonesian Journal of Science and Technology, 2019;4(1): 97-118.doi:10.17509/ijost.v4i1.15806

[26] Hossain T, Alam MA, Rahman MA, Sharafat MK, Minami H, Gafur MA, Ahmad H, Zwitterionic poly (2-(methacryloyoxy) ethyl phosphprylcholine) coated mesoporous silica particles and doping with magnetic nanoparticles. Colloids and Surfaces. A:Physicochemical and Engineering Aspects. 2018;555:80-87. https://doi.org/10.1016/j.colsurfa.2018.06.020

[27] Sarker MZ, Rahman MM, Minami H, Suzuki T, Ahmad H. Amine functional silica-supported bimetallic Cu-Ni nanocatalyst and investigation of some typical reductions of aromatic nitro substituents. Colloid and Polymer Science. 2022; 1:1-8

[28] Nayak PS, Singh BK. Instrumental characterization of clay by XRF, XRD and FTIR, Bulletin of Materials Science. 2007;30(3). 235-238. http://dx.doi.org/10.1007/s12034-007-0042-5

[29] Sadri N, Baghernejad M, Ghasemi-Fasaei R, Moosavi AA, Hardie AG. Characterization of clay and nanoclay extracted from a semi-arid Vertisol and Investigation of their carbon sequestration potential. Environmental Monitoring and Assessment. 2024;196(1):96. doi:10.1007/s10661-023-12246-x. PMID: 38153593

[30] Onyekonwu MO, Ogolo NA. Investigating the use of nanoparticles in enhancing oil recovery. InSPE Nigeria Annual International Conference and Exhibition 2010; SPE-140744.

[31] Rezvani H, Binks BP, Ngugen D, Surfactant-Nanoparticles Formulations for Enhanced Oil Recovery in Calcite-Rich Rocks. Langmuir: the ACS journal of surfaces ad colloids, 2024; 40(47):24989-25002. https://doi.org/10.1021/acs.langmuir.4c03100.

[32] Konne JL, Udeh OV, Cookey, GA, & Nmegbu GCJ. Surfactant (Sodium Dodecyl Sulphate) Coated Silica (SiO_2) Nanoparticles for Enhanced Oil Recovery: An Optimized Approach. Iranian Journal of Oil and Gas Science and Technology. 2022; 11(2): 65-80. doi:10.22050/ijogst.2022.334848.1632.

[33] Al-Anssari S, Arif M, Wang S, Barifcani A, Iglauer S Stabilizing nanofluids in saline environments. Journal of Colloid Interface Science. 2017; 508, 222–229. https://doi.org/10.1016/j.jcis.2017.08.043